The Effect Of Nb Doping On $LiNiO_2$ (101) Surface: DFT+U Study

M. Hiine[1*], P.E. Ngoepe[1] & K.P. Maenetja[1]

ARTICLE INFO

Article details
Presented at the 26th annual conference of the Rapid Product Development Association of South Africa, held from 27 to 30 October 2025 in Pretoria, South Africa

Available online 8 Dec 2025

Contact details
* Corresponding author
jassicon11@gmail.com

Author affiliations
1 Materials Modelling Centre, University of Limpopo, South Africa

ORCID® identifiers
M. Hiine
https://orcid.org/0000-0003-4811-9927

P.E. Ngoepe
https://orcid.org/0000-0003-0523-5602

K.P. Maenetja
https://orcid.org/0000-0002-3199-0946

DOI
http://dx.doi.org//10.7166/36-3-3347

ABSTRACT

Doping nickel-rich layered metal oxides is a key strategy to enhance the structural stability and performance of lithium-ion battery cathodes. Niobium (Nb) has a larger ionic radius, and higher valence can stabilise the NiO_2 lattice and suppress undesired phase transition. This study uses spin-polarised DFT + U-D3(BJ) calculations to investigate the effect of Nb doping on the (101) surface of $LiNiO_2$, focusing on the first and second layers. Nb doping improves the crystal lattice and reduces volume change. It also lowers surface free energies compared with the undoped surface, indicating enhanced surface stability. Notably, doping in the second layer stabilises the surface more effectively than in the first layer. Bader charge analysis shows a lower charge on Nb in the first layer, while a higher work function in the first layer suggests greater reactivity. Ethylene carbonate (EC) adsorption on Ni sites of both doped and pristine surfaces yields negative adsorption energies, confirming thermodynamic stability. Among all sites, Ni_{23} shows the most negative adsorption energy, suggesting the strongest interaction with EC. This study reveals layer-dependent effects of Nb doping and their impact on EC adsorption, providing guidance for designing more stable and efficient $LiNiO_2$ cathodes.

OPSOMMING

Die dotering van nikkelryke gelaagde metaaloksiede is 'n sleutelstrategie om die strukturele stabiliteit en werkverrigting van litiumioonbatterykatodes te verbeter. Niobium (Nb) het 'n groter ioniese radius, en hoër valensie kan die NiO_2-rooster stabiliseer en ongewenste fase-oorgang onderdruk. Hierdie studie gebruik spin-gepolariseerde DFT + U-D3(BJ) berekeninge om die effek van Nb-dotering op die (101)-oppervlak van $LiNiO_2$ te ondersoek, met die fokus op die eerste en tweede lae. Nb-dotering verbeter die kristalrooster en verminder volumeverandering. Dit verlaag ook oppervlakvrye energieë in vergelyking met die ongedoteerde oppervlak, wat dui op verbeterde oppervlakstabiliteit. Dit is opmerklik dat dotering in die tweede laag die oppervlak meer effektief stabiliseer as in die eerste laag. Bader-ladingsanalise toon 'n laer lading op Nb in die eerste laag, terwyl 'n hoër werkfunksie in die eerste laag groter reaktiwiteit suggereer. Etileenkarbonaat (EC)-adsorpsie op Ni-plekke van beide gedoteerde en ongerepte oppervlaktes lewer negatiewe adsorpsie-energieë, wat termodinamiese stabiliteit bevestig. Onder al die plekke toon Ni23 die mees negatiewe adsorpsie-energie, wat die sterkste interaksie met EC aandui. Hierdie studie onthul laagafhanklike effekte van Nb-dotering en hul impak op EC-adsorpsie, wat leiding bied vir die ontwerp van meer stabiele en doeltreffende $LiNiO_2$-katodes.

1. INTRODUCTION

The demand for lithium-ion batteries (LIBs) with high energy capacity, especially to power electronics and electric vehicles, has driven major efforts to improve battery materials. The cathode, which is the heaviest and most expensive part of these batteries, is a key focus for boosting battery capacity [1]. Since the 1980s, cathode materials such as $LiMO_2$ have been widely studied [2]. Among these, nickel-rich layered oxides are seen as the most promising for next-generation LIBs owing to their high energy density (over 800 Wh/kg) and capacity (around 200 mAh/g) [3, 4, 5].

However, $LiNiO_2$ faces issues with poor cycling stability, primarily because of oxygen loss and structural instability, particularly when used at high voltages [6]. Significant efforts such as surface coatings [7], doping [8], and core-shell hierarchical structures [9] have been used to enhance the structural stability and electrochemical performance of Ni-rich $LiNiO_2$ cathodes. Doping is regarded as an effective strategy to enhance the electrochemical performance of LNO positive electrode material, with cation doping at Ni sites being one of the most effective methods [10].

The stabilisation process classifies the effects of cation doping into two categories: (i) doping with low-valent metals such as Mg, Cu, Al, etc., which can either stabilise the valence of the Ni ion or induce electrostatic repulsion [11, 12, 13], potentially reducing cation mixing and hindering the migration of Ni^{2+} ions from the transition-metal slab to the Li slab during electrochemical cycles; and (ii) the stabilisation process involving doping with high-valent metals such as Ti, Mo, and Nb [14, 15, 16], often introduces increased complexity. Nonetheless, the electrochemical cycling stability of $LiNiO_2$ remains an issue.

To maintain the high capacity of $LiNiO_2$, it is preferable to use methods that make minimal alterations to the original structure to optimise its performance. In this context, re-evaluating the impact of simple single-element cation doping on the stability and performance of $LiNiO_2$ is valuable [17]. Niobium (Nb) is a highly favoured dopant for various LIB cathode materials because of its low cost and atomic mass. Nb-doping has been shown to improve the structural and thermal stability of nickel-rich materials [18]. However, previous studies have not fully explored how Nb doping affects different surface layers, surface stabilisation, or interactions with electrolytes, which is the focus of this study. Here, we use spin-polarised DFT+U calculations to investigate Nb-doping effects on $LiNiO_2$ (101) surface layers and analyse EC adsorption, providing insights into layer-dependent stability and electrolyte interactions not addressed in previous studies.

2. COMPUTATIONAL METHODOLOGY

Spin-polarised density functional theory (DFT) calculations as implemented in the Vienna Ab-initio Simulation Package (VASP) was used to calculate the surface of $LiNiO_2$ [19]. All computations were performed using the Perdew, Burke, and Ernzerhof (PBE) exchange-correlation function within the generalised gradient approximation (GGA) [20]. The Kohn-Sham (KS) valence state expansion has a fixed kinetic energy cut-off of 500 eV, which ensures the convergence of total energies and forces for the $LiNiO_2$ surface. To integrate all surfaces in the reciprocal space, a 4x4x1 k-point Monkhorst-Pack grid with the origin as the Γ-center was used, which was sufficient to sample accurately the Brillouin zone for the surface supercell while keeping computational cost reasonable. In the application of Kresse and Joubert [21], the core electrons and their interaction with the valence electrons were modelled using the projector augmented wave (PAW) approach [22]. The levels up to the 3d orbital for nickel and the 1s orbital for carbon and oxygen make up the core electrons, while all the electrons are classified as valence electrons for lithium and hydrogen. Our calculations also used the semi-empirical approach of Grimme with the Becke-Johnson damping [D3-(BJ)] [23, 24] to model the long-range dispersion interactions, which are necessary to represent surfaces adequately. During geometry improvements, gaussian smearing with a width of 0.05 eV was set to enhance the convergence of the Brillioun zone integrations [24]. To achieve precise electrical and magnetic characteristics as well as total energies, the tetrahedron approach with Blöchl corrections was used [22]. The Hubbard adjustment [25] was used to enhance the description of the localised 3d Ni electrons in the formulation of Dudarev *et al.* [26]. We used the effective parameter U_{eff} = 6.0 eV, which is consistent with the values in the literature, and has been shown to reproduce accurately the electronic structure of Ni-based layered oxides [27, 28, 29].

3. RESULTS AND DISCUSSION

3.1. Surface free energies

Here, we discuss the effect of surface doping with Nb on the Ni atom(s) in the top and second layers. In order to examine the impact of surface doping, we calculated the surface free energy for the changed surfaces, specifically for Nb-doped surfaces, using the following formula:

$$\sigma = \gamma_r + \frac{E_{LiNiNbO_2} + E_{Ni_2} - E_{LiNiO_2} - E_{Nb}}{A} \quad (1)$$

where γ_r is the surface energy for the relaxed pristine $LiNiO_2$ surface, E_{Nb} is the energy of the Nb-doped $LiNiO_2$ surface, and E_{LiNiO_2} is the energy of the relaxed pristine. The slab model consisted of eight atomic layers, with the bottom four layers fixed and the top four layers allowed to relax; a vacuum region of 15 Å was included to prevent interactions between periodic images.

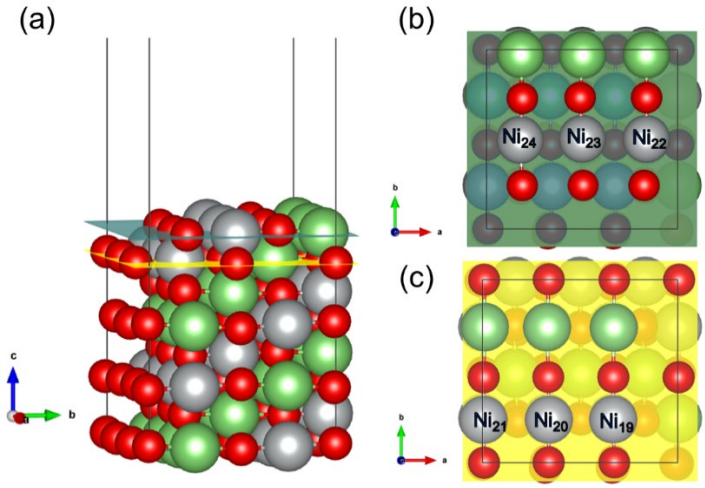

Figure 1: (a) Side and (b), (c) top views showing the two top layers considered for niobium/manganese doping on layered $LiNiO_2$ (101) surface

The surface free energies (σ) for single Nb-doped surfaces on the top and second layers of $LiNiO_2$ are summarised in Table 1. When a Nb atom is doped on to the top layer, the Ni_{22} (0.057 eV/Å²) site exhibits a lower surface free energy than the Ni_{23} (0.067 eV/Å²) and Ni_{24} (0.060 eV/Å²) sites. This suggests that the presence of Nb has a more significant stabilising effect on the Ni_{22} site than Ni_{23} and Ni_{24}. In contrast, when Nb is doped into the second layer of the $LiNiO_2$ surface, the Ni_{19} (0.041 eV/Å²) site shows a lower surface free energy than the Ni_{20} (0.052 eV/Å²) and Ni_{21} (0.063 eV/Å²) sites, indicating that Nb has a stronger stabilising impact on the Ni_{19} site, making it less reactive. In addition, the second layer, when doped with Nb, shows a 15.93% decrease in surface free energy compared with the top layer, suggesting that Nb in the second layer has a more pronounced surface-stabilising effect.

Table 1: Surface free energy (σ) for the single Nb doped on first and second layers of $LiNiO_2$

Doping layers	Doping sites	σNb (eV/Å²)
Top-layer	Ni_{22}	0.057
	Ni_{23}	0.067
	Ni_{24}	0.060
Sub-surface layer	Ni_{19}	0.041
	Ni_{20}	0.052
	Ni_{21}	0.063

Moreover, the surface free energies for single Nb doping are lower than the surface energy of the pristine $LiNiO_2$ (101). This implies that Nb doping on the $LiNiO_2$ surface contributes to stabilising the pristine $LiNiO_2$ (101) surface, enhancing its overall stability.

3.2. Density of state

In order to correlate the structural and mechanical stability of the Nb-doped and pristine surface of $LiNiO_2$ (101), we compared their total density of states (tDOS) plots in Figure 2. It was noted from the literature that the DOS of structures of the same composition can be used to mimic the stability trend with respect to their behaviour at the E_f (Fermi level), in which the structure with the highest and lowest density of states at E_f is considered the least and most stable respectively [30].

In our spin-resolved analysis, the spin-up channel shows that the pristine surface has a lower DOS around E_f than the Nb-doped surface, indicating greater stability for the pristine surface in this channel. In the spin-down channel, the Nb-doped surface with Nb in the second layer exhibits the lowest DOS, while both the top-layer Nb-doped and the pristine surfaces show negligible DOS. This indicates that the Ni d-orbitals are fully occupied and do not contribute to the DOS at E_f, suggesting the reduced availability of electronic states for surface reactions.

Therefore, changes in the spin-down DOS reflect how Nb doping modifies the surface electronic structure and potentially influences surface reactivity. Our DOS analyses are consistent with the stability trend predicted by the surface free energies. At the Fermi level, the DOS of the pristine and first-layer Nb-doped surface is ~0.0 states/eV, while the second-layer Nb-doped surface is ~-30 states/eV, further illustrating the difference in stability between the configurations. Therefore, the spin-resolved DOS supports the conclusion that Nb doping, particularly in the second layer, enhances the stability of the $LiNiO_2$ (101) surface.

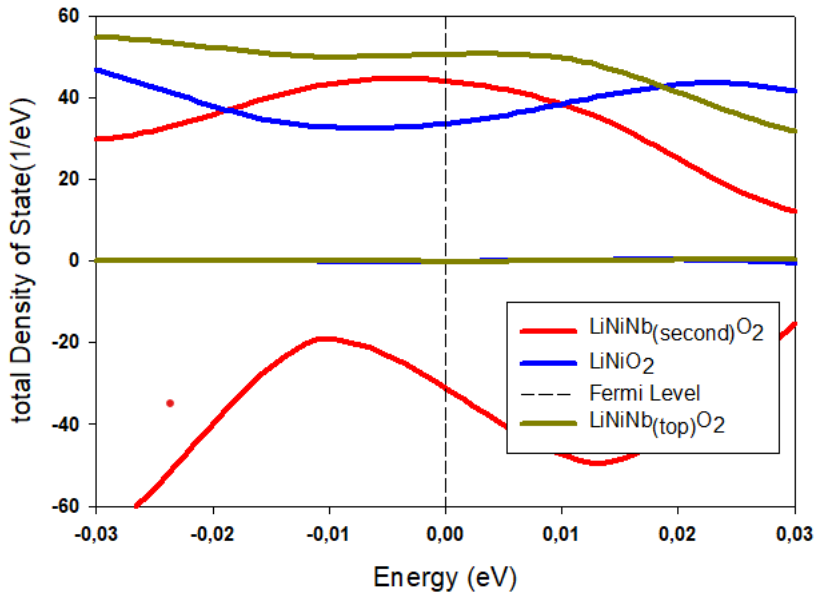

Figure 2: Total density of states for Nb-doped surfaces and pristine surface for $LiNiO_2$ (101) surfaces

3.3. Bader charges analysis

Table 2 presents the electronic charge transfer (Δq) analysis following Nb doping on $LiNiO_2$ surfaces, alongside their corresponding work functions (ϕ). The charge transfer is indicative of electron accumulation (negative charge) or depletion (positive charge). For Nb-doped surfaces, the highest charge depletion of 2.6 e− was observed on the second layer Nb atom. This was coupled with charge accumulation of -0.208 e− and -0.113 e− on the neighbouring Ni atoms Ni_{20} and Ni_{21} respectively. This analysis helped to highlight the impact of Nb doping on the electronic properties of $LiNiO_2$ surfaces, particularly in relation to charge distribution and reactivity.

Table 2: Bader charge analysis for the Nb doping (q(Nb)) on the first and second layers of the $LiNiO_2$ (101) surface alongside their neighbouring Ni atomic charges (q (Ni)Neigb) and work functions (ϕ)

	Doping layers	q(Nb) (e-)	q(Ni)Neigb (e-)		ϕ (eV)
			Ni1	Ni2	
Nb-doping	1st layer	2.400	-0.216	-0.209	5.232
	2nd layer	2.600	-0.208	-0.113	5.281

Furthermore, we calculated the work function that the energy required to remove an atom to the vacuum, using the equation:

$$\phi = E_{\mathrm{vac}} - E_{\mathrm{F}} \quad (2)$$

where E_{vac} and E_F are the surface electrostatic potential energy and the Fermi level respectively.

For the Nb-doped surfaces, doping in the second layer resulted in a higher work function (ϕ = 5.281 eV), suggesting that the second-layer doped surface was less reactive than the first layer. As the positive charge on the Nb ions in the second layer increased, the work function also increased. In addition, the average charge on the neighbouring atoms showed an increase when doping occurred on the second layer of the $LiNiO_2$ surface, indicating a shift in the overall electronic properties and reactivity of the material.

3.4. Ethylene carbonate adsorption

This section discusses the effect of the adsorption of the electrolyte component, ethylene carbonate (EC), on the Nb-doped $LiNiO_2$ (101) surface, compared with the pristine surface. EC is the most widely used solvent in commercial Li-ion battery electrolytes, and is known to strongly interact with layered oxide cathodes, including $LiNiO_2$. Initially, the energy of the EC molecule was calculated and found to be -61.974 eV. EC was then adsorbed on various Ni positions in the top layer of both the doped and the pristine surfaces. The adsorption energy (Ead) of EC on these surfaces was determined with the following equation:

$$E_{ad} = E_{sys} - (E_{surf} + E_{EC}) \quad (3)$$

where E_{sys} corresponds to the total energy of the adsorption system, E_{surf} corresponds to the total energy of the $LiNiO_2$ (101) slab, and E_{EC} corresponds to the total energy of an isolated EC molecule.

In the simulations, the EC molecule was initially positioned at distances of 1.907 Å and 2.070 Å from the Nb and Ni sites on the surface respectively. These initial distances were chosen to be close enough to allow strong interaction between the EC molecule and the surface cations while avoiding unphysical overlap of electron densities. This configuration was chosen to favour attractive interactions over repulsive ones between the EC molecule and the surface. Both the adsorbate and the surface were allowed to move and adjust their geometry during the optimisation process, enabling the system to reach a stable adsorption configuration.

The adsorption of EC was examined on both the pristine and the Nb-doped $LiNiO_2$ (101) surfaces at different Ni positions (Ni_{22}, Ni_{23}, and Ni_{24}). The adsorption energy varied depending on the Ni position. Nb doping resulted in the stronger adsorption energy than the pristine surface, with the highest energy observed when EC was adsorbed on the Nb-doped Ni_{23} position (-3.127 eV). The adsorption energy changed from Ni_{22} to Ni_{24} for both the pristine and the Nb-doped surfaces. The pristine surface displayed weaker adsorption energies than the doped surface.

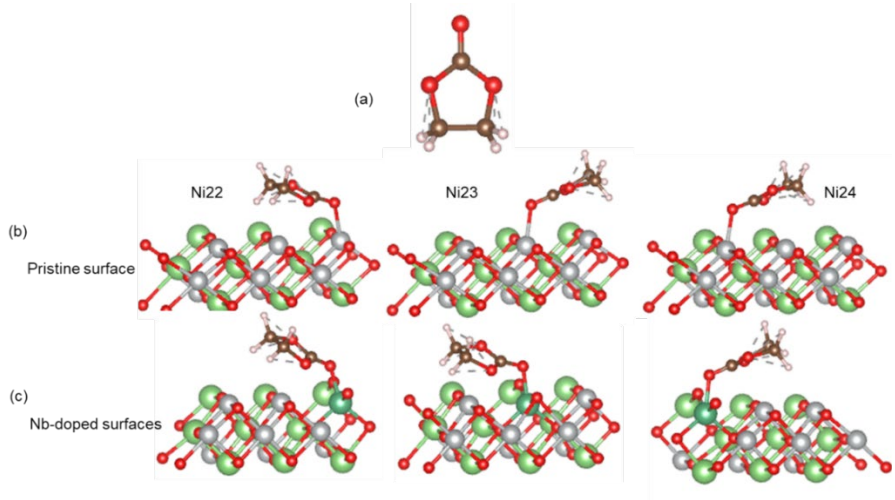

Figure 3: (a) EC molecule, (b) EC adsorbed on pristine $LiNiO_2$ (101) surface on Ni sites, (c) EC adsorbed on Nb-doped on $LiNiO_2$ (101) surface on Ni site

Table 3 presents the adsorption energies of EC on pristine and doped $LiNiO_2$ (101) surfaces, highlighting the influence of doping on adsorption strength. The adsorption energy of EC on the pristine surface is weaker in all nickel positions (Ni_{22}, Ni_{23}, and Ni_{24}), indicating a lower affinity for EC because of the less reactive nature of undoped nickel sites. In contrast, doping significantly enhances adsorption, with Nb doping leading to more negative adsorption energies, signalling stronger EC–surface interactions. The strong adsorption at Ni_{23} in the Nb-doped surface could be attributed not only to Nb's larger atomic radius and higher valence but also to the local surface geometry and electronic environment. Ni_{23} is coordinated in a way that allows optimal overlap of EC orbitals with surface states, and the local electronic density favours stronger adsorption interactions.

Table 3: Calculated adsorption energies (Ead) of EC molecule on pristine and Nb/Mn-doped on $LiNiO_2$ (101) surface

Surface type	Doping position	Adsorption site	Adsorption energy (eV)
Pristine	-	Ni_{22}	-1.100
	-	Ni_{23}	-1.120
	-	Ni_{24}	-0.976
Nb-doped	Ni_{22}	Ni_{22}	-2.677
	Ni_{23}	Ni_{23}	-3.127
	Ni_{24}	Ni_{24}	-2.909

4. CONCLUSION

The DFT method was used to explore the effects of Nb doping on $LiNiO_2$ (101) and its interaction with EC. Nb doping on the second layer was found to result in a lower surface free energy than doping on the top layer, indicating a greater stabilising effect when Nb occupies subsurface positions. In the spin-up state, the pristine surface exhibited a lower density of states around the Fermi level than the Nb-doped surface, suggesting enhanced stability for the pristine configuration. In the spin-down state, the second-layer Nb-doped surface exhibited the lowest density of states, whereas the pristine and top-layer doped surfaces showed negligible states, indicating fully occupied Ni d-orbitals. Nb doping in the second layer also led to an increased work function (ϕ = 5.232 eV), indicating reduced surface reactivity. Furthermore, EC adsorption was stronger on both the pristine and the Nb-doped Ni_{23} surfaces (-1.120 eV and -3.027 eV respectively), suggesting that Nb doping at the Ni_{23} site enhances surface reactivity and interaction strength with the electrolyte. These results imply that Nb doping, particularly in subsurface layers, can enhance surface stability and electrolyte interactions, which may improve the cycling performance and durability of $LiNiO_2$ cathodes in lithium-ion batteries.

ACKNOWLEDGEMENTS

The calculations were performed at the Materials Modelling Centre (MMC) at the University of Limpopo and the Centre for High Performance Computing (CHPC) in Cape Town. The authors acknowledge the National Research Foundation (NRF) for its financial support. The authors also thank the University of Limpopo for academic support.

This research was supported by the National Research Foundation (NRF) of South Africa under PMDS22061523262.

REFERENCES

[1] **S.L. Dreyer, P. Kurzhals, S.B. Seiffert, P. Müller, A. Kondrakov, T. Brezesinski, and J. Janek**, "The effect of doping process route on $LiNiO_2$ cathode material properties," *Journal of The Electrochemical Society*, vol. 170, no. 6, 060530, 2023. https://doi.org/10.1149/1945-7111/acdd21

[2] **S. Muto, K. Tatsumi, Y. Kojima, H. Oka, H. Kondo, K. Horibuchi, and Y. Ukyo**, "Effect of Mg-doping on the degradation of $LiNiO_2$-based cathode materials by combined spectroscopic methods," *Journal of Power Sources*, vol. 205, pp. 449–455, 2012. https://doi.org/10.1016/j.jpowsour.2012.01.071

[3] **Y.-K. Sun**, "Future of electrochemical energy storage," *ACS Energy Letters*, vol. 2, no. 3, 716, 2017. https://doi.org/10.1021/acsenergylett.7b00158

[4] **J. Xu, F. Lin, M.M. Doeff, and W. Tong**, "A review of Ni-based layered oxides for rechargeable Li-ion batteries," *Journal of Materials Chemistry A*, vol. 5, pp. 874–901, 2017. https://doi.org/10.1039/C6TA07991A

[5] **C.S. Yoon, D.-W. Jun, S.-T. Myung, and Y.-K. Sun**, "Structural stability of $LiNiO_2$ cycled above 4.2 V," *ACS Energy Letters*, vol. 2, pp. 1150–1155, 2017. https://doi.org/10.1021/acsenergylett.7b00304

[6] **J. Cheng, B. Ouyang, and K.A. Persson**, "Mitigating the high-charge detrimental phase transformation in $LiNiO_2$ using doping engineering," *ACS Energy Letters*, vol. 8, pp. 2401–2407, 2023. https://doi.org/10.1021/acsenergylett.3c00169

[7] **Y. Zhang, H. Li, J. Liu, J. Liu, H. Ma, and F. Cheng**, "Enhancing $LiNiO_2$ cathode materials by concentration-gradient yttrium modification for rechargeable lithium-ion batteries," *Journal of Energy Chemistry*, vol. 63, pp. 312–319, 2021. https://doi.org/10.1016/j.jechem.2021.07.029

[8] **P. Mohan, G. Paruthimal Kalaignan, and V.S. Muralidharan**, "Improved the electrochemical performance of $LiCe_{1-x}Ni_xO_2$ cathode material for rechargeable lithium ion battery," *Journal of Nanoscience and Nanotechnology*, vol. 12, no. 9, pp. 7052–7059, 2012. https://doi.org/10.1166/jnn.2012.6510

[9] **J. Zhang, Z. Yang, R. Gao, L. Gu, Z. Hu, and X. Liu**, "Suppressing the structure deterioration of Ni-rich $LiNi_{0.8}Co_{0.1}Mn_{0.1}O_2$ through atom scale interfacial integration of self-forming hierarchical spinel layer with Ni gradient concentration," *ACS Applied Material & Interfaces*, vol. 9, pp. 29794–29803, 2017. https://doi.org/10.1021/acsami.7b08802

[10] **L. Wang, Y.-G. Sun, L.-L. Hu, J.-Y. Piao, J. Guo, A. Manthiram, J. Ma, and A.-M. Cao**, "Copper substituted $Na_{0.67}Ni_{0.3-x}Cu_xMn_{0.7}O_2$ cathode materials for sodium-ion batteries with suppressed P2–O2 phase transition," *Journal of Materials Chemistry A*, vol. 5, pp. 8752–8761, 2017. https://doi.org/10.1039/C7TA00880E

[11] **G. Li, Z. Zhang, R. Wang, Z. Huang, Z. Zuo, and H. Zhou**, "Effect of trace Al surface doping on the structure, surface chemistry and low temperature performance of $LiNi_{0.5}Co_{0.2}Mn_{0.3}O_2$ cathode," *Electrochimica Acta*, vol. 201, pp. 399–407, 2016. https://doi.org/10.1016/j.electacta.2016.07.033

[12] **Q.N. Sa, J.A. Heelan, Y. Lu, D. Apelian, and Y. Wang**, "Copper impurity effects on $LiNi_{1/3}Mn_{1/3}Co_{1/3}O_2$ cathode material," *ACS Applied Materials & Interfaces*, vol. 7, pp. 20585–20590, 2015. https://doi.org/10.1021/acsami.5b04426

[13] **A. Milewska, M. Molenda, and J. Molenda**, "Structural, transport and electrochemical properties of $LiNi_{1-y}Co_yMn_{0.1}O_2$ and Al, Mg and Cu substituted $LiNi_{0.65}Co_{0.25}Mn_{0.1}O_2$ oxides," *Solid State Ionics*, vol. 192, pp. 313–320, 2011. https://doi.org/10.1016/j.ssi.2010.11.026

[14] **Y. Zhang, Z.B. Wang, F.D. Yu, L.F. Que, M.J. Wang, Y.F. Xia, Y. Xue, and J. Wu**, "Studies on stability and capacity for long-life cycle performance of $Li(Ni_{0.5}Co_{0.2}Mn_{0.3})O_2$ by Mo modification for lithium-ion battery," *Journal of Power Sources*, vol. 358, pp. 1–12, 2017. https://doi.org/10.1016/j.jpowsour.2017.05.013

[15] **X. Yuan, Q.J. Xu, X. Liu, W. Shen, H. Liu, and Y. Xia**, "Excellent rate performance and high capacity of Mo doped layered cathode material $Li[Li_{0.2}Mn_{0.54}Ni_{0.13}Co_{0.13}]O_2$ derived from an improved coprecipitation approach," *Electrochimica Acta*, vol. 207, pp. 120–129, 2016. https://doi.org/10.1016/j.electacta.2016.04.180

[16] **X. Feng, Y. Gao, L. Ben, Z. Yang, Z. Wang, and L. Chen**, "Enhanced electrochemical performance of Ti doped $Li_{1.2}Mn_{0.54}Co_{0.13}Ni_{0.13}O_2$ for lithium-ion batteries," *Journal of Power Sources*, vol. 317, pp. 74–80, 2016. https://doi.org/10.1016/j.jpowsour.2016.03.101

[17] **H. Cao, F. Du, J. Adkins, Q. Zhou, H. Dai, P. Sun, D. Hu, and J. Zheng**, "Al- doping induced superior lithium-ion storage capability of $LiNiO_2$ spheres," *Ceramics International*, vol. 46, pp. 20050–20060, 2020. https://doi.org/10.1016/j.ceramint.2020.05.078

[18] **U.H. Kim, S.-T. Myung, C.S. Yoon, Y.-K. Sun**, "Extending the battery life using an Al doped $Li[Ni_{0.76}Co_{0.09}Mn_{0.15}]O_2$ cathode with concentration gradients for lithium-ion batteries," *ACS Energy Letters*, vol. 2, pp. 1848–1854, 2017. https://doi.org/10.1021/acsenergylett.7b00613

[19] **G. Kresse and J. Furthmüller**, "Efficient iterative schemes for *ab initio* total energy calculations using a plane wave basis set," *Physical Review B*, vol. 54, pp. 11169–11186, 1996. https://doi.org/10.1103/PhysRevB.54.11169

[20] **J.P. Perdew, K. Burke, and M. Ernzerhof**, "Generalized gradient approximation made simple," *Physical Review Letters*, vol. 77, pp. 3865–3868, 1996. https://doi.org/10.1103/PhysRevLett.77.3865

[21] **G. Kresse and D. Joubert**, "From ultrasoft pseudopotentials to the projector augmented-wave method," *Physical Review B*, vol. 59, pp. 1758–1775, 1999. https://doi.org/10.1103/PhysRevB.59.1758

[22] **P.E. Blöchl**, "Projector augmented-wave method," *Physical Review B*, vol. 50, pp. 17953–17979, 1994. https://doi.org/10.1103/PhysRevB.50.17953

[23] **S. Grimme, S. Ehrlich, and L. Goerigk**, "Effect of the damping function in dispersion corrected density functional theory," *Journal of Computational Chemistry*, vol. 32, pp. 1456–1465, 2011. https://doi.org/10.1002/jcc.21759

[24] **S. Grimme, J. Antony, S. Ehrlich, and H. Krieg**, "A consistent and accurate *ab initio* parametrization of density functional dispersion correction (DFT D) for the 94 elements H–Pu," *The Journal of Chemical Physics*, vol. 132, 154104, 2010. https://doi.org/10.1063/1.3382344

[25] **V.I. Anisimov, M.A. Korotin, J. Zaanen, and O.K. Andersen**, "Spin bags, polarons, and impurity potentials in $La_{2-x}Sr_xCuO_4$ from first principles," *Physical Review Letters*, vol. 68, pp. 345–348, 1992. https://doi.org/10.1103/PhysRevLett.68.345

[26] **S.L. Dudarev, G.A. Botton, S.Y. Savrasov, C.J. Humphreys, and A.P. Sutton**, "Electron energy loss spectra and the structural stability of nickel oxide: An LSDA + U study," *Physical Review B*, vol. 57, pp. 1505–1509, 1998. https://doi.org/10.1103/PhysRevB.57.1505

[27] **M. Tuccillo, O. Palumbo, M. Pavone, A.B. Muñoz García, A. Paolone, and S. Brutti**, "Analysis of the phase stability of $LiMO_2$ layered oxides (M = Co, Mn, Ni)," *Crystals*, vol. 10, 526, 2020. https://doi.org/10.3390/cryst10060526

[28] **L. Wang, T. Maxisch, and G. Ceder**, "Oxidation energies of transition metal oxides within the GGA + U framework," *Physical Review B*, vol. 73, 195107, 2006. https://doi.org/10.1103/PhysRevB.73.195107

[29] **X. Li, Q. Wang, H. Guo, N. Artrith, and A. Urban**, "Understanding the onset of surface degradation in $LiNiO_2$ cathodes," *ACS Applied Energy Materials*, vol. 5, pp. 5730–5741, 2022. https://doi.org/10.1021/acsaem.2c00012

[30] **R. Mahlangu, M.J. Phasha, H.R. Chauke, and P.E. Ngoepe**, "Structural, elastic and electronic properties of equiatomic PtTi as potential high-temperature shape memory alloy," *Intermetallics*, **F**vol. 33, pp. 27–32, 2013. https://doi.org/10.1016/j.intermet.2012.09.021